Global Change Biology

Global Change Biology (2012) **18**, 2594–2605, doi: 10.1111/j.1365-2486.2012.02681.x

Long-term carbon storage through retention of dissolved aromatic acids by reactive particles in soil

MARC G. KRAMER*, JONATHAN SANDERMAN†, OLIVER A. CHADWICK‡, JON CHOROVER§ and PETER M. VITOUSEK¶

*Department of Earth and Planetary Sciences, University of California, High Street, Santa Cruz, CA 95064, USA, †Division of Land and Water, CSIRO, Urrbrae, SA 5064, Australia, ‡Department of Geography, University of California, Santa Barbara, CA 93106, USA, §Department of Soil, Water and Environmental Science, University of Arizona, Tucson, AZ 85721, USA, ¶Department of Biology, Stanford University, Stanford, CA 94305, USA

Abstract

Soils retain large quantities of carbon, thereby slowing its return to the atmosphere. The mechanisms governing organic carbon sequestration in soil remain poorly understood, yet are integral to understanding soil-climate feedbacks. We evaluated the biochemistry of dissolved and solid organic carbon in potential source and sink horizons across a chronosequence of volcanic soils in Hawai'i. The soils are derived from similar basaltic parent material on gently sloping volcanic shield surfaces, support the same vegetation assemblage, and yet exhibit strong shifts in soil mineralogy and soil carbon content as a function of volcanic substrate age. Solid-state ^{13}carbon nuclear magnetic resonance spectra indicate that the most persistent mineral-bound carbon is comprised of partially oxidized aromatic compounds with strong chemical resemblance to dissolved organic matter derived from plant litter. A molecular mixing model indicates that protein, lipid, carbohydrate, and char content decreased whereas oxidized lignin and carboxyl/carbonyl content increased with increasing short-range order mineral content. When solutions rich in dissolved organic matter were passed through Bw-horizon mineral cores, aromatic compounds were preferentially sorbed with the greatest retention occurring in horizons containing the greatest amount of short-range ordered minerals. These minerals are reactive metastable nanocrystals that are most common in volcanic soils, but exist in smaller amounts in nearly all major soil classes. Our results indicate that long-term carbon storage in short-range ordered minerals occurs via chemical retention with dissolved aromatic acids derived from plant litter and carried along preferential flow-paths to deeper B horizons.

Keywords: aromatic acids, carbon cycle science, climate change, dissolved organic carbon, long-term carbon stabilization, short range ordered minerals, soil carbon, soil minerals

Received 17 May 2011; revised version received 30 November 2011 and accepted 10 December 2011

Introduction

Mineral-associated organic matter accumulates in soils enriched in colloids derived from weathering of primary silicates. Short-range ordered (SRO) metastable colloidal solids, in particular, strongly sorb, and stabilize soil organic matter (SOM) (Torn *et al.*, 1997) as exemplified by the disproportionate sequestration of C in the particularly SRO-mineral rich soils formed from volcanic ejecta. These soils occupy only 0.8% of the global land area but store as much as 5% of the global soil C pool (Dahlgren *et al.*, 2004).

Short-range ordered minerals are reactive metastable nanocrystals that form from weathering of framework silicates and ferromagnesian minerals, parent minerals that are found in most rocks from granites to basalts to sandstones and siltstones. The largest quantities of SRO minerals are found in volcanic soils, but smaller amounts exist in soils representing all major soil classes across a broad range of parent material and climates (Fig. 1 and Supporting materials references). SRO minerals have high surface area with large numbers of hydroxyl groups, and are one of the most chemically active inorganic components of soil. Even small amounts of these minerals provide an important substrate for sorbing organic compounds within soil.

Carbon that accumulates in mineral soil may originate from a variety of sources. Although there has recently been increasing consensus that most stabilized C has been highly processed by microbial assimilation and turnover (Kögel-Knabner *et al.*, 2008; Sollins *et al.*, 2009; Kleber & Johnson, 2010) other possible sources include root tissue and exudates, the formation and persistence

Present address: Marc G. Kramer, US Forest Service, Portland, OR, 97208, USA.

Correspondence: Marc G. Kramer, tel. + 415 608 8712, fax + 510 559 5679, e-mail: mkramer@ucsc.edu

of char (Kleber & Johnson, 2010) or direct translocation and subsequent stabilization of plant-derived compounds, such as lignin, from litter leachate (Kaiser & Guggenberger, 2000; Guggenberger & Kaiser, 2003). Despite recent improvements in our understanding of C stabilization mechanisms in mineral soils, prediction of the precise sources, pathways and ultimate fate of sequestered C remains a major challenge in terrestrial biogeochemistry research (Sollins *et al*., 1996; Kaiser & Guggenberger, 2000; Guggenberger & Kaiser, 2003; Kalbitz & Kaiser, 2008; Kögel-Knabner *et al*., 2008). Such knowledge is critical for evaluation of the magnitude and direction of feedbacks between rising temperatures of the atmosphere and the vast reservoir of soil C (Davidson & Janssens, 2006). Here we consider the extent to which the interaction between dissolved organic matter (DOM) derived from plant litter and SRO minerals exerts a primary control on long-term carbon storage.

Our work builds on previous studies which have examined organic matter composition, turnover time, and soil mineralogy (e.g., Torn *et al*., 1997; Chorover *et al*., 1999, 2004; Mikutta *et al*., 2009, 2010; Marin-Spiotta *et al*., 2011) along a well-studied chronosequence of volcanic soils in Hawai'i. These previous studies highlighted the role of SRO minerals in long-term OM retention, however the source for C accumulation in the subsoil and the mechanism for its retention remained unclear. One of these studies (Mikutta *et al*., 2009) identified aromatic acids and SRO minerals in close association in the subsoil of intermediate aged sites. Here we elucidate the source and chemical nature of these compounds and the mechanisms for retention using naturally occurring stable isotopes, nuclear magnetic resonance, and soil column leaching experiments.

Materials and methods

We sampled soil profiles to weathered rock or to ~1 m depth along a chronosequence of volcanic soils in Hawai'i. The soils are derived from similar basaltic parent material on gently sloping volcanic shield surfaces whose ages are 0.3, 20, 150, 350, 1400, and 4100 ky with similar climate (MAT = 16 °C and MAP = 2500 mm). The ecosystems on these surfaces support the same vegetation assemblage and hence similar organic decomposition products, and yet exhibit strong shifts in soil mineralogy and soil carbon content as a function of age (Vitousek, 2004) (Table 1). Vegetation is dominated by Ohi'a trees (*Metreosida polymorpha*) with numerous ferns and herbaceous plants in the understory. Net primary productivity and nutrient availability across the chronosequence is lowest at the youngest (0.3 ky) and oldest (4100 ky) sites, and highest at the intermediate aged sites (20 –350 ky). Chemically reactive SRO minerals extracted using ammonium oxalate as a chelating agent comprise from 2% to 68% of the soil mass with the highest values occurring at depths between 50 and 100 cm in the intermediate aged sites (20 ky–350 ky).

Solid-state ^{13}C-nuclear magnetic resonance (NMR) spectroscopy was combined with C and nitrogen (N) elemental and stable isotope analyses to compare the composition of subsoil SOM with DOM derived from the forest-floor organic layer. A molecular mixing model constrained by C:N ratios (Nelson & Baldock, 2005) was then applied to NMR regions to estimate biomolecular composition. Organic and mineral soil horizon leaching experiments were conducted in the lab to assess if the DOM derived from plant litter could be a direct source for mineral-soil carbon accumulation the subsoil.

Soil sampling

At all field sites, soils were sampled by genetic horizon to weathered rock or to about 1 m in depth. Soil classifications for each of the six sites are as follows: (1) Lithic Hapludand (Thurston Site), (2–4) Aquic Hydrudand (Laupahoehoe, Kohala, Pololu Sites), (5) Aquic Hapludand (Kolekole Site), and (6) Plinthic Kandiudox (Kokee Site). Samples from each of the organic and mineral horizons were collected using standard

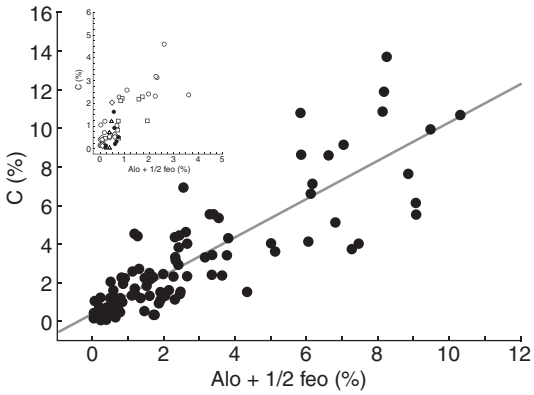

Fig. 1 The distribution of SRO minerals and soil C content from soils worldwide. As relative SRO mineral abundance increases, soil C content increases ($P < 0.01$, $r^2 = 0.72$, $n = 126$). SRO mineral abundance was estimated by using Alo + ½ Feo content (%). Data from 126 published B mineral soil horizons worldwide including Oxisol, Alfisol, Mollisol, Podzol, Andisol soil orders (See Supporting materials references for data used in Fig. 1 and for additional references that report a positive Feo, Alo: C relationship). Inset A: Even for non-volcanic soils (Oxisol, Ultisol, Alfisol, Inceptisol soils) SRO mineral content is tightly coupled to soil C content ($P < 0.01$, $r^2 = 0.63$, $n = 58$). Hollow circles = Oxisol soil order. Hollow square = Inceptisol soil order, Hollow diamond = Alfisol soil order. Hollow triangle = Mollisol soil prder, Black solid circle = Ultisol. References used for Fig. 1 are (Stutzer, 1998; Delvaux *et al*., 2004; Bäumler *et al*., 2005; Rasmussen *et al*., 2005, 2007; Buurman *et al*., 2007; Sanderman *et al*., 2008; Igwe *et al*., 2009). See Supporting materials for additional references that support a positive Alo:C, Feo:C relationship.

Table 1 Selected soil properties, including %C, %N, C/N, $\delta^{15}N$, $\Delta^{14}C$ [$\Delta^{14}C$ from (Torn *et al.*, 1997) and new data acquired in this MS for Pololu] and SRO mineral abundance, with depth across the chronosequence: Site A) Thurston 300y, Site B) Laupahoehoe 20 ky, Site C) Kohala 150 ky, Site D) Pololu 350 ky, Site E) Kolekole 1.4 My, Site F) Kokee 4.1 My. Bw mineral horizons used in Fig. 9b, B and A horizons used in the core leaching experiment shown in boldface type

Site	Horizon designation	Mineral sample no.	Depth (cm)	C (%)	N (%)	C/N	$\delta^{15}N$ (‰)	$\Delta^{14}C$ (‰)	SRO minerals (%)
Thurston 0.3 ky	Oie		0–4	51.6	1.2	43	−4.5		
	Oa		4–10	36.8	1.3	28	−3.1	202.8	
	A	1	10–18	8.4	0.5	16	−0.7	144.3	9
	Bw	**2**	**18–26**	**1.8**	**0.1**	**17**	**1.5**	**98.9**	**12**
	2Ab	3	26–29	4.5	0.3	16	2.2	2.91	10
	2Bwb	**4**	**29–35**	**4**	**0.3**	**16**	**1.8**	**−4.09**	**9**
Laupahoehoe 20 ky	Oie		0–5	51.4	1.4	37	1.6	15.75	
	Oa		5–12	33.8	1.5	23	2.9	194.3	
	Ag or Bh	5	12–20	32.8	1.8	18	5.9	−0.32	14
	Bg or Bhs	**6**	**20–27**	**15.7**	**0.7**	**22**	**5.6**	**−205**	**19**
	Bw1	7	27–39	10.8	0.39	28	4.3	−224	35
	Bw2	8	39–52	10.7	0.37	29	4.6	−318	25
	Bw3	**9**	**52–71**	**10.8**	**0.34**	**32**	**3.2**	**−426**	**50**
	Bw4	10	71–94	9.9	0.31	32	3.5	−582	55
Kohala 150 ky	Oie		0–2	41.8	1.8	23	0.0		
	Oa		2–4	33.3	1.77	19	2.6	198.1	
	Ag or Bh	11	4–11	20.6	1.56	13	3.1	−35.3	7
	Bg or Bhs	12	11–21	3.9	0.47	8	4.7	−178	4
	Bw1	13	21–48	8.6	0.29	29	4.1	−386	38
	Bw2	14	48–78	9.1	0.25	37	2.8	−823	32
	Cr1	15	78–100	7.6	0.19	40	1.3	−916	33
Pololu 350 ky	Oie		0–7	42.8	1	45	−0.8		
	Oa		7–15	45.7	1.9	24	4.0	—-	
	Ag or Bh	16	15–25	22.1	1.2	18	4.1	1.8	1
	Bg or Bhs	**17**	**25–31**	**13.6**	**0.8**	**18**	**3.9**	**—-**	**3**
	Bw1	18	31–46	13.7	0.36	38	1.6	—-	43
	Bw2	**19**	**46–62**	**11.9**	**0.32**	**37**	**1.9**	**−565**	**40**
	B3	20	62–80	9.5	0.32	30	1.3	—-	45
	Cr	21	80+	8.6	0.26	33	1.7	—-	68
Kolekole 1.4 My	Oie		0–2	47.5	1.7	27	−1.5		
	Oa		2–10	35.9	1.6	22	0.9	262.4	
	Ag or Bh	22	10–21	22.3	1.33	17	5.5	24.25	13
	Bg or Bhs	**23**	**21–30**	**12.6**	**0.8**	**16**	**4.0**	**−32.4**	**14**
	Bw1	24	31–38	7.6	0.42	18	4.2	−197	14
	Bw2	25	38–58	1.5	0.06	24	4.2	−303	26
	Bw3	**26**	**58–72**	**1.1**	**0.04**	**28**	**3.7**	**−486**	**23**
Kokee 4.1 My	Oie		0–2	52.91	2.18	24	1.4		
	Oa		2–7	48.42	2.06	24	2.8	193.4	
	Ag	27	7–11	14.76	0.65	23	2.9	142.4	5
	Bhs	28	11–16	3.56	0.14	25	2.9	−724	3
	Bw1	**29**	**16–23**	**2.36**	**0.09**	**27**	**3.2**	**−104**	**4**
	Bw2	30	23–32	3.17	0.09	34	5.0	−320	6
	Bw3	31	32–43	2.56	0.15	17	5.7	−459	4
	Bw4	32	43–54	2.25	0.22	10	6.0	−648	5
	Bw5	**33**	**54–72**	**1.2**	**0.07**	**17**	**6.1**	**−821**	**5**

US soil survey diagnostic criteria (Schoeneberger *et al.*, 1998). Air-dried samples were sieved (2-mm mesh) to remove large organic and mineral particles. A 1-mm sieve was used to further pick out large organic particles including roots, bark, and other identifiable plant parts.

Quantitation of short-range order minerals

Short-range order minerals were quantified as part of a series of progressively harsher chemical extractions of the < 2-mm soil material (Chadwick *et al.*, 2003). After removal of organic

matter and organically bound aluminium (Al) and Iron (Fe) with hydrogen peroxide (H_2O_2), the residue was extracted using 0.275 M ammonium oxalate, pH 3.25, 1 : 100 soil:extractant (Burt, 2004). Ammonium oxalate selectively removes short-range ordered hydrous oxides of Fe and Al such as allophane and ferrihydrite, but is a poor extractant of imogolite and layer silicates and does not extract crystalline hydrous oxides of Fe and Al, opal, or crystalline silicate (Wada, 1989). Most commonly Fe, Al, and silicon (Si) in the supernatant are measured as an indicator of SRO mineral quantity (i.e. Fig. 1), but in this case the mass of SRO mineral was determined by recording weight loss after extraction (Torn *et al*., 1997; Vitousek *et al*., 1997; Chadwick *et al*., 2003).

Carbon, N and ^{15}N analyses

Carbon, N and $\delta^{15}N$ were measured with a coupled continuous-flow elemental analyzer-isotope ratio mass spectrometer (EA-IRMS) system with a Carlo-Erba model 1108 EA (Carlo Erba Strumentazione, Milan, Italy) interfaced to a Thermo-Finnigan Delta Plus XP IRMS (Thermo Fisher Scientific, Waltham, MA, USA). Dry samples (<2 mm) were ground finely with a zirconium mortar and pestle, and loaded into tin boats. Stable isotope data are reported relative to atmospheric air for ^{15}N: $\boldsymbol{\delta}^{15}N = (R_{sample} - R_{std})/R_{std} \times 1000$. Precision of in-house standards, which had been calibrated using international standards, was typically better that 0.2 per mil for $\boldsymbol{\delta}^{15}N$. One standard was run for every 10 unknowns, and two blanks and conditioning and calibration standards were included at the beginning and end of each run. Samples were run in duplicate and were always within the range of the standards. Analysis of internal standards indicated an analytical error of <5% for N and <2% for C. Samples were analyzed at the light stable isotope facility of the University of California, Santa Cruz.

NMR analysis

Solid State ^{13}C cross-polarization magic-angle spinning (CP/MAS) NMR data were recorded with a Bruker AVANCE500 (Bruker Daltonics Inc., Billerica, MA, USA) spectrometer equipped with an 11.74T magnet (Bruker Daltonics Inc., Billerica, MA, USA). Soil samples were ground to a powder and then loaded in a 4 mm zirconia rotor with Kel-F end cap. DOM (1–2 L) was obtained by collecting leachates from weekly irrigation during the organic soil core leaching experiment and compositing solution from the same core. Dissolved organic C samples were first distilled to 30 ml of high DOM-concentration solution using a rotary evaporator under high vacuum at 50 °C. These solution samples were then lyophilized and prepared in the same manner as the soil samples for NMR analysis. NMR Larmor frequencies for ^{13}C and 1H were 125 and 500 MHz. The rotor was spun at 15 kHz to eliminate the spinning sidebands. A CP pulse sequence with ramped-amplitude mixing power and a two-pulse-phase-modulated (TPPM) decoupling technique was used, the contact time was 1 ms, the recycle delay was 1 s, the spectrum width was 500 KHz. Identical acquisition parameters were used on all samples. Spectra were smoothed with a line broadening of 100 Hz and further compared against a range of other 50 and 200 Hz line broadening settings (Table S1). Spin counting on samples was used to compare amount of C observed against pure glycene reference standards. Because the C content of these samples was sufficiently high (>4% C) no hydrofluoric acid chemical pre-treatment was used, thus avoiding any possible preferential removal of carboxyl C from bulk soil samples (Dai & Johnson, 1999; Schilling & Cooper, 2004; Hockaday *et al*., 2009). Only soil samples that contained $\geq 4\%$ C (Table 1), had a signal:noise ratio >20, and >30% NMR observable C were considered to be interpretable, resulting in inclusion of mineral samples#1, 3–23 (22/33 total) (Table 1). Direct polarization (DP) experiments on samples with high C observability (>85%) were conducted to confirm the relative shifts of aromatic and carboxyl regions observed in the CPMAS Spectra (Table S2). Spin counting with a glycene reference standard and background rotor subtraction were performed on the DP NMR spectra. Spectral intensities for each sample were determined by integrating signal intensities in seven chemical shift region regions: 0–45, 45–60, 60–95, 95–110, 110–145, 145–165, and 165–215 ppm. Because NMR peaks obtained on the mineral samples were too broad to allow assignment of chemical components directly, we applied a C and N constrained 6-component molecular mixing model to ^{13}C CPMAS NMR spectral regions to estimate biochemical components (carboxyl-carbonyl C, char, lignin, lipid, protein, carbohydrate). Van Krevelen plots using molar ratios of H:C and O:C were generated using molecular mixing model results, which predict C, H, O, N elemental ratios as well as biochemical components. Model details and limitations can be found in Baldock *et al*. (2004) and Nelson & Baldock (2005). To quantitate the biochemical similarity/dissimilarity between sites and sample types, a principle components analysis was conducted using PRIMER 6 software (Clarke & Gorley, 2006) on the distribution of signal intensity across the seven major chemical shift regions for vegetation (leaf and root material), soil (Oie, Oa, A, and Bw horizons) and DOM (O core leachates) samples from all sites.

Soil column leaching experiments

Column experiments were designed by placing replicated (n = 3) intact O horizons, and Oie and Oa sub-horizons, into 10 cm I.D. ABS cores fitted with a draining end-cap containing a glass fiber filter (Whatman GF/D) and 5 cm length of acid-washed pre-combusted glass wool to aid in drainage. Cores were irrigated weekly with 30–50 mm of simulated rainwater (pH = 6.4, ionic strength = 1.78×10^{-4} mol dm^{-3}, DOC = 1.1 mg C L^{-1}, total N = 0.3 mg N L^{-1}, with the following mean concentrations (μM): Ca = 9.9, Fe = 1.0, Mg = 2.0, Na = 106, Si = 38.2, Cl = 25.5, NO_3 = 0.5, SO_4 = 4.3) using low-flow mist sprayers.

Three replicates of mineral (A and B) soil horizons were placed into identical 10 cm ABS cores. They were repacked to original bulk density using either measured horizon thickness (Table 1) or 10 cm soil material if the horizon was thicker than 10 cm. A standard composite mixture of all the O-horizon effluents was then gravity fed through the mineral cores at weekly intervals (250–300 ml of solution per week). Biweekly

respiration measurements on both organic and mineral cores were made by continuous monitoring of the change in CO_2 concentration within the headspace for 5–10 min using a dynamic flow-through cap connected to an infra-red gas analyzer (PP Systems, Amesbury, MA, USA).

Solution samples were collected immediately (within 2 h) after irrigating, passed through Whatman GX/D 0.45 μm filters (Whatman International Ltd, Maidstone, Kent, UK), and refrigerated. Dissolved organic carbon content was determined on a Shimadzu TOC-V_{CSH} analyser (Shimadzu, Kyoto, Japan). Ultraviolet light absorption was measured on a single-beam Shimadzu 1600 UV/Vis Spectrophotometer (Shimadzu). Specific UV absorption (SUVA, L mg C^{-1} m^{-1}), used here as a proxy for relative aromaticity of a sample (Weishaar *et al.*, 2003), was calculated as the absorption at 254 nm normalized to DOC concentration. Bioavailability of O horizon DOM was determined on samples obtained 2 months into the experiment using the rapid determination (7 days) protocol with added nutrients (McDowell *et al.*, 2006). Oxalate extractable organic carbon released into solution during SRO mineral dissolution was determined by measuring dissolved organic carbon (DOC) in solution and then subtracting out the background oxalate C concentration. Carbon and SRO mineral dissolution in deionized water was used as a control.

Results

NMR measurements (by NMR region) were plotted against SRO mineral abundance and are shown in Fig. 2. Carboxyl C and aromatic C increased with increasing SRO mineral abundance (Fig. 2a, b). By contrast, both O-alkyl and alkyl content decreased with SRO mineral abundance (Fig. 2c and d). The NMR spectra of the subsoil organic matter bears strong chemical resemblance to that of DOM derived from plant litter (Fig. 3; Table 1). Despite the similarity to litter-derived DOM, the subsoil organic matter is much older and more resistant to decomposition than that in the near-surface horizons (Table 1).

Consistent with the NMR results, the NMR-based molecular mixing model constrained by C and N elemental measurements indicates protein, lipid, carbohydrate, and char content decreased whereas lignin and carboxyl/carbonyl C content increased with increasing SRO mineral content (Fig. 4). Van Krevelen plots examining molar ratios of H:C and O:C derived from the mixing model showed increased aromaticity and oxidation with increasing SRO mineral abundance, indicating that the lignin fragments are highly degraded and oxidized (Fig. 5).

Stable isotope soil depth profiles showed a trend of gradual N isotope enrichment with depth (at the youngest (0.3 ky) and oldest (4100 ky) sites along the chronosequence (Fig. 6). At the intermediate aged sites (20–350 ky) the $\delta^{15}N$ values increased with depth from the top of the soil profile values to a depth of 30 cm (to the Ah horizon) but then became progressively more depleted with depth. The depleted $\delta^{15}N$ values and

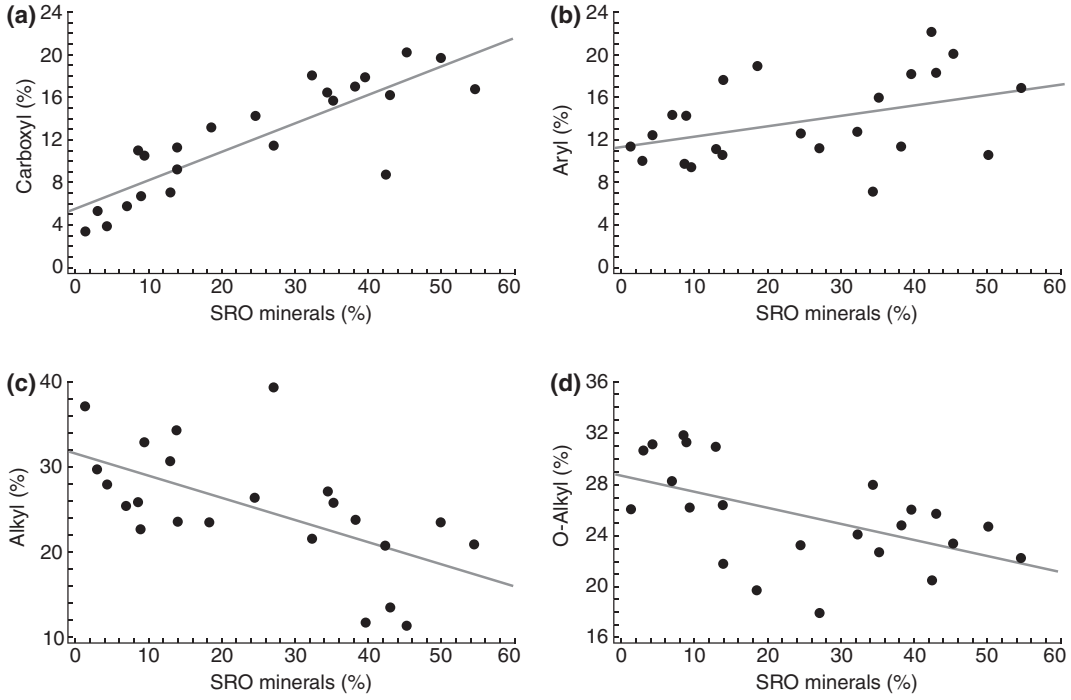

Fig. 2 Changes in relative proportions of major NMR regions as a function of SRO mineral abundance in mineral soil horizons across the chronosequence. (a) SRO:Carboxyl ($P < 0.01$; $r^2 = 0.73$, $n = 22$), (b) SRO:Aryl ($P < 0.05$; $r^2 = 0.18$, $n = 22$. (c) SRO:Alkyl ($P < 0.05$; $r^2 = 0.37$, $n = 22$), (d) SRO:O-Alkyl ($P < 0.05$; $r^2 = 0.29$, $n = 22$).

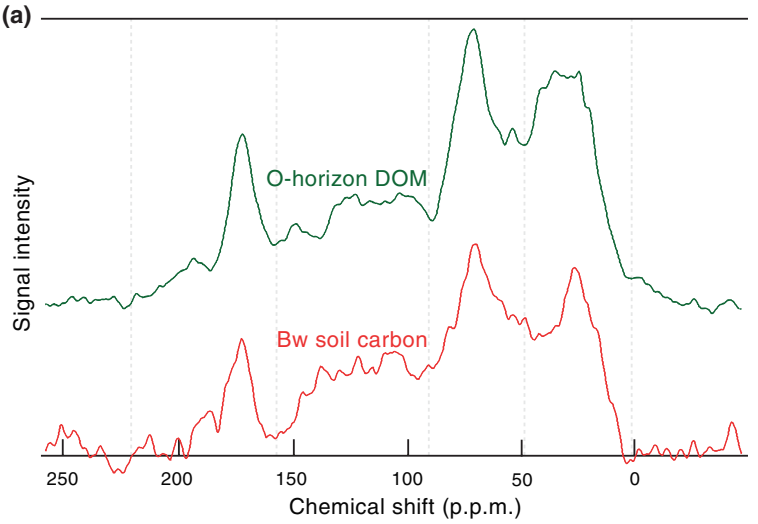

Chemical shift (p.p.m.)	0–45 (%)	45–60 (%)	60–95 (%)	95–110 (%)	110–145 (%)	145–165 (%)	165–210 (%)
O-Horizon DOM	29	6	25	6	13	6	14
Bw soil carbon	21	12	22	6	17	5	17

Biochemical component	Carbohydrate (%)	Protein (%)	Lignin (%)	Lipid (%)	Carbonyl (%)	Char (%)
O-horizon DOM	26	12	32	18	14	0
Bw soil carbon	21	8	34	13	21	3

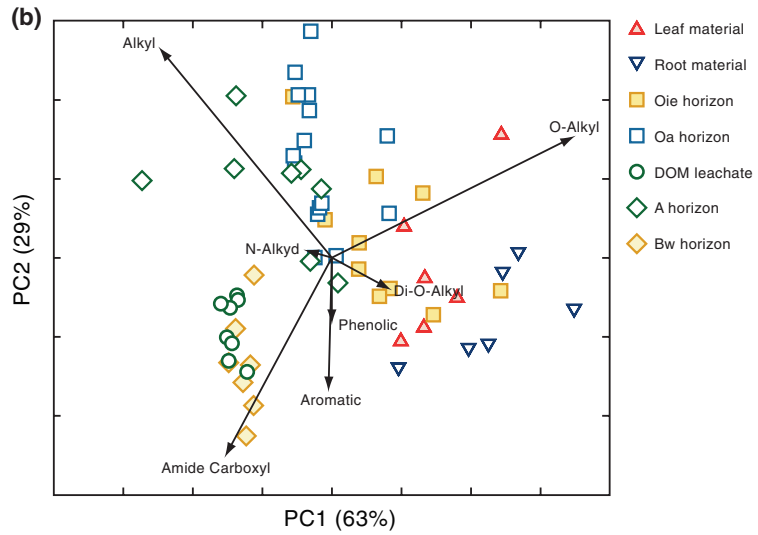

Fig. 3 (a) Solid-state ^{13}C NMR spectra of plant-litter DOM and Bw-horizon soil carbon with high SRO mineral abundance [Lapahoehoe (20 ky) Site]. Proportions of chemical shift regions are shown in inset below. A molecular mixing model (Baldock *et al.*, 2004) applied to the NMR spectra showing major biochemical compounds from each is shown in the inset. (b) Principal component analysis showing statistical similarity between DOM and Bw soil carbon from intermediate aged (20–350 ky) chronosequence sites when compared against other C sources across the chronosequence. Eigenvectors show each NMR shift region influence on principle components. Aromatic and carboxyl C NMR regions explain much of the statistical similarity between DOM and Bw. Samples were from DOM generated in soil column leaching experiment, major diagnostic organic and mineral horizons and select root samples across the chronosequence.

high C/N ratios in the deeper Bw soil horizons, where SRO mineral abundance is high are similar to those of undecomposed (Oie) plant litter values, indicating that these materials have undergone minimal microbial processing (Figs 6 and 7; Table 1) (Kramer *et al.*, 2003; Dijkstra *et al.*, 2008).

To determine how much DOM was retained with SRO minerals present in the subsoil, we quantitatively

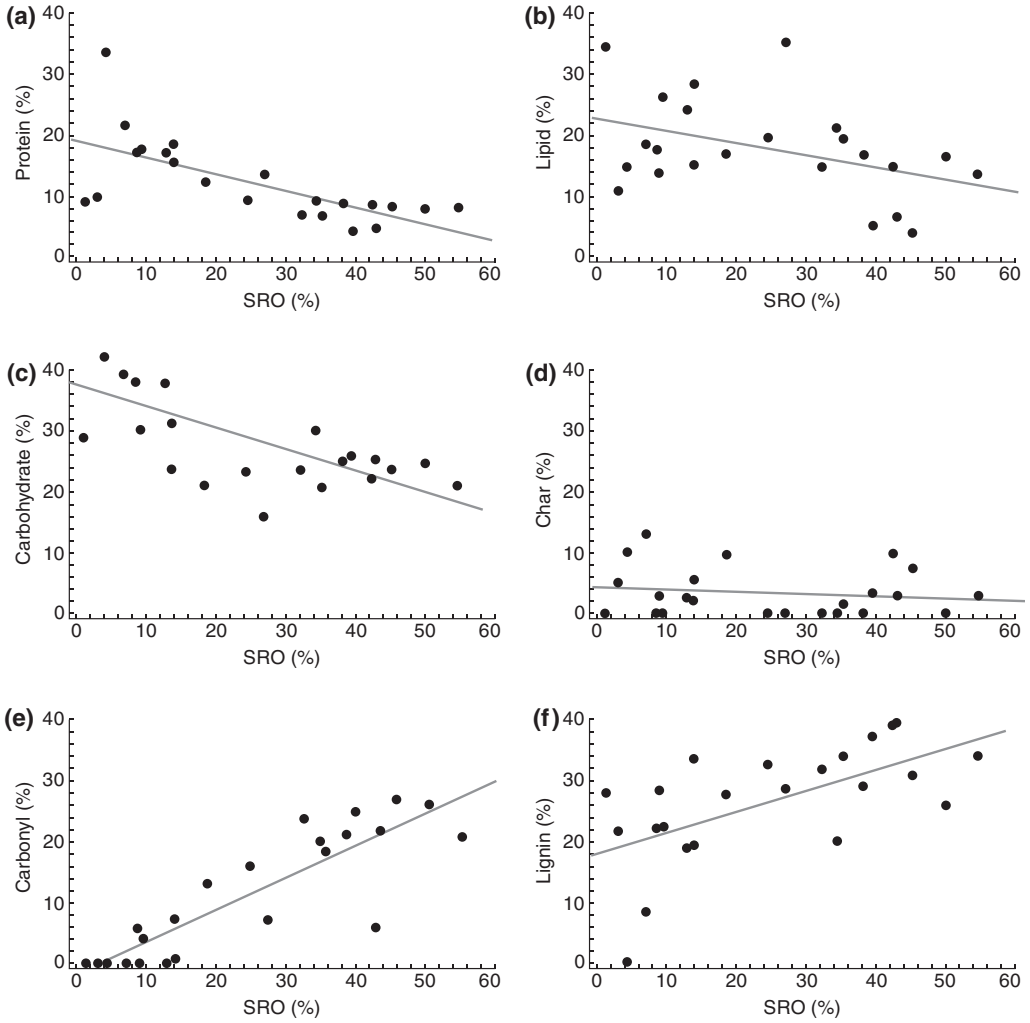

Fig. 4 Changes in biochemical components as a function of SRO mineral abundance in mineral soil horizons across the chronosequence. (a) SRO:Protein ($P < 0.05$, $r^2 = 0.46$, $n = 22$) (b) SRO:Lipid ($P < 0.05$, $r^2 = 0.18$, $n = 22$) (c) SRO:Carbohydrate ($P < 0.05$, $r^2 = 0.76$, $n = 22$) (d) SRO:Char ($P > 0.05$) (e) SRO:Carbonyl ($P < 0.05$, $r^2 = 0.76$, $n = 22$) (f) SRO:Lignin ($P < 0.05$, $r^2 = 0.38$, $n = 22$).

measured carbon released into solution during oxalate acid treatment and the C content in remaining soil mass following the treatment. On average, 64% (SE 3, $n = 25$) of the total soil C content was released following dissolution of SRO minerals and that the amount of DOC released (mg C g^{-1} soil) was a function of SRO mineral content (Fig. 8). By contrast <5% of total C was lost in the deionized water control.

Soil column leaching experiments were conducted to further assess if the DOM derived from plant litter could be the source for carbon accumulation in the deeper (Bw) mineral soil horizons. The amount of DOM produced from organic soil horizons on a per gram substrate basis varied across the chronosequence (Fig. 9a), and was highest in the intermediate-aged (20 ky) nutrient rich soils that also have high rates of net primary productivity (NPP) and microbial activity (Vitousek, 2004). Solid-state ^{13}C NMR spectra and specific UV absorption (SUVA) measurements show that the DOM leached from the organic horizons was rich in carboxyl and aromatic fragments rather than carbohydrates or other labile compounds that would be more rapidly consumed by microbes (Fig. 2a). A subsequent bioavailability experiment confirmed that most of the DOM leaching from the organic horizons was not readily degradable (6–10% DOM loss over a 7 day period). However, tight coupling between DOM production and microbial activity, as measured by soil respiration on a per gram substrate basis, strongly suggests that solubilisation and high production rates of this less degradable DOM were nonetheless influenced substantially by microbial activity (Fig. 9a).

When identical DOM-rich solutions derived from organic horizons was leached through Bw-horizon

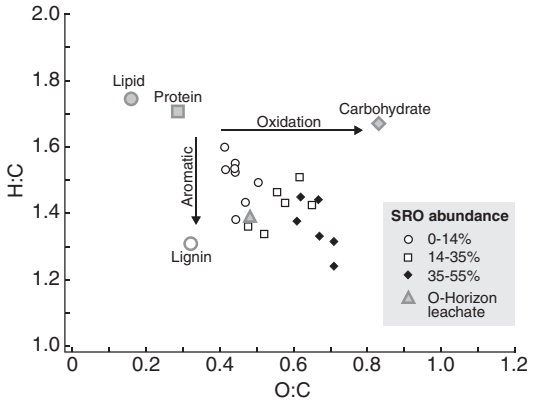

Fig. 5 van Krevelen plot showing H:C and O:C molar ratios from mineral soil horizon samples across the chronosequence plotted against theoretical values for lipid, carbohydrates, protein and lignin. Increasingly oxidized and aromatic compounds were found to preferentially accumulate with increasing SRO mineral abundance. Hollow circles = 0–14% SRO abundance, Hollow squares = 14–35% SRO mineral abundance, solid black diamonds = 35–55% SRO abundance.

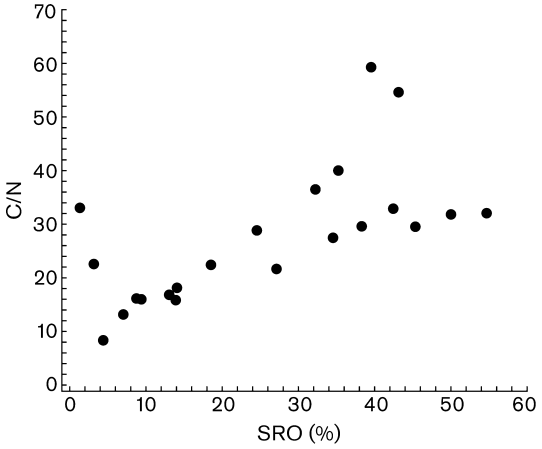

Fig. 7 Relationship between C/N ratio and SRO mineral abundance in mineral soil horizons across the chronosequence. SRO mineral abundance (%): C/N ratio, $P < 0.1$, $r^2 = 0.45$, $n = 33$.

mineral cores, SUVA and DOC measurements of the effluent DOM showed preferential retention of aromatic compounds with the greatest retention occurring in soil columns containing the highest SRO mineral abundance (Fig. 9b). This result complements previous characterization of solid phase mineral-organic complexes along the chronosequence (Mikutta *et al.*, 2009). By contrast, in A horizons where SRO mineral abundance is low, our SUVA data indicated no preferential sorption of aromatic compounds. Desorption, although minimal, was negatively correlated with the concentration of SRO minerals.

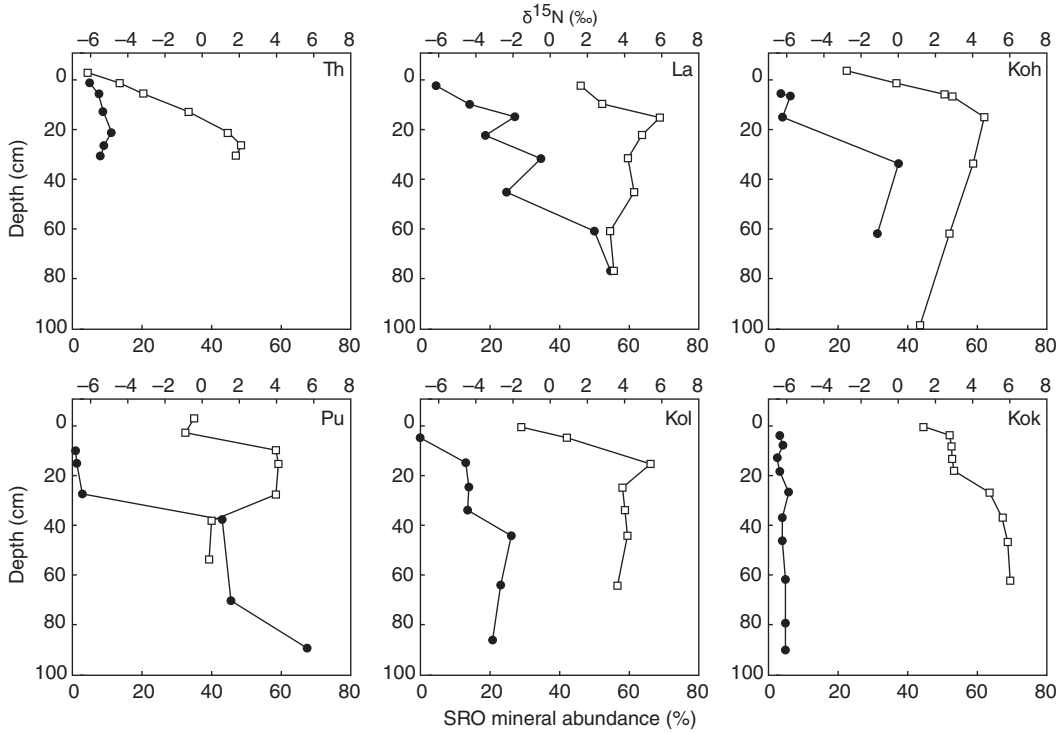

Fig. 6 Soil depth profiles of $\delta^{15}N$ and SRO minerals across the chronosequence. Chronosequence Site Th) Thurston 300y, Site La) Laupahoehoe 20 ky, Site Koh) Kohala 150 ky, Site Pu) Pololu 350 ky, Site Kol) Kolekole 1.4 My, Site Kok) Kokee 4.1 My. $\delta^{15}N$ = hollow squares. SRO minerals = black circles.

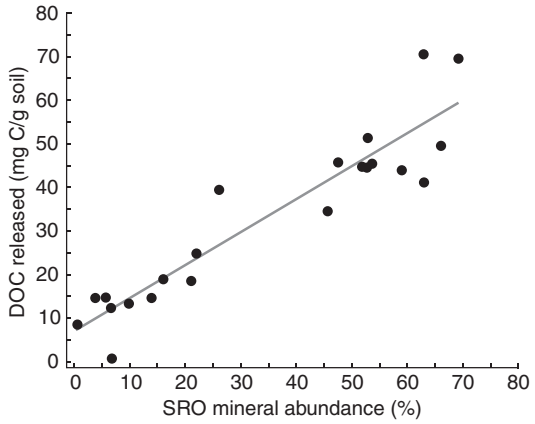

Fig. 8 The amount of carbon released from soil as DOC after SRO mineral dissolution with acid oxalate extraction. Samples were from Bw mineral horizons across the chronosequence (Table 1) $P < 0.01$, $r^2 = 0.87$, $n = 22$.

Results from the NMR spectroscopy (Figs. 2, 4 and 5), the ^{15}N isotopic and C and N elemental measurements (Figs 6 and 7; Table 1), and the soil column leaching experiment (Fig. 9), and previously reported radiocarbon ^{14}C ages (Table 1) (Torn *et al*., 1997) indicate that the oldest and most persistent C stores across the chronosequence are comprised of partially oxidized aromatic plant compounds which are a close chemical match to dissolved organic matter (Fig. 3).

Discussion

Collectively, our results suggest that DOM comprised largely of aromatic acids accumulated preferentially with SRO minerals present in the subsoil. The soil column leaching experiments and NMR data (Figs 2, 3, 4, 5 and 9) indicate that DOM derived from plant litter is the source for this material. The correlation between aromatic acids and SRO minerals (Figs 2, 3 and 5) and the soil column sorption experiments (Fig. 9) suggest that chemical retention via binding (sorption) to soil minerals through reactive OH sites is the dominant mechanism, although other retention mechanisms such as co-precipitation or structural retention are also possible (Parfitt, 2009; Chevallier *et al*., 2010). Structural retention could occur by preferential microbial consumption of carbohydrates or alkyl-rich compounds with residual organic acids accumulating in mesopores (2–50 nm) (Chevallier *et al*., 2010). However, that mechanism does not explain the clear association of oxidized aromatics and SRO minerals (Figs 2a, b and 5) and does not account for the control of SRO mineral dissolution on the amount of soil carbon released as DOC (Fig. 8). Co-precipitation would not explain the high rates of

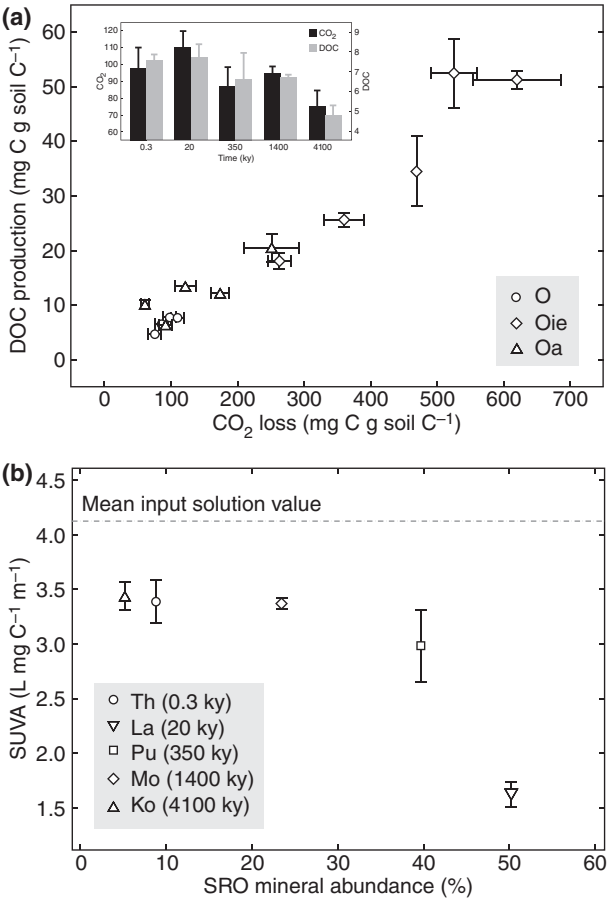

Fig. 9 (a) Organic soil horizon DOC production and microbial activity in the soil column leaching experiment across all chronosequence sites over 5 months of cumulative DOM production (Inset) $P < 0.01$, $r^2 = 0.95$, $n = 15$. Hollow diamond = Oie-subhorizons. $P < 0.001$, $r^2 = 0.68$, $n = 5$. Hollow triangle = Oa-subhorizons $P < 0.01$, $r^2 = 0.57$, $n = 5$. Hollow circles = Whole-O horizons. $P < 0.01$, $r^2 = 0.59$, $n = 5$. (b) SUVA values show aromatic compounds were preferentially retained in all soil sorption columns and was strongest in the soil column with the highest SRO mineral content. Starting input DOM solution (leachate from the organic cores) was identical for all cores (mean SUVA = 4.11 ± 0.11 L mg C^{-1} m^{-1}). Error bars represent 1 SE. ($n = 15$). Sites shown include Thurston, Laupahoehoe, Pololu, and Kolekole, and Kokee.

sorption observed in the soil column leaching experiment.

The formation of carboxyl-rich compounds as oxidation products of plant-derived biomolecules such as lignin and associated phenolic substances has long been considered an important pathway for DOM production and potentially for organic matter accumulation in soil (Waksman & Tenney, 1928; Martin *et al*., 1980; Kirk & Farrell, 1987; Shevchenko & Bailey, 1996; Kaiser & Guggenberger, 2000; Kalbitz & Kaiser, 2008). Our results demonstrate the long-term accumulation of

such plant-derived compounds in direct association with SRO minerals.

During microbial breakdown of fresh plant materials, cellulose, and carbohydrates are preferentially utilized over lignin (Martin *et al*., 1980). Highly oxidized lignin polyphenols, tannins, and other recalcitrant plant-derived compounds are partly solubilized and mobilized by peroxidase and ligninase enzymes (Kirk & Farrell, 1987; Shevchenko & Bailey, 1996), but the resulting carboxyl-rich ring structures are more resistant to microbial biodegradation (Kalbitz *et al*., 2006). As a constituent of DOM, oxidized and aromatic plant fragments can bind directly to hydroxylated mineral surfaces, or into pre-existing mineral-organic complexes. In either case, carboxyl and phenolic functional groups bind to exposed metal centers (Kaiser & Guggenberger, 2000; Chorover & Amistadi, 2001).

In contrast to the accumulation of oxidized aromatic plant compounds at depth, highly processed organic matter (alkyl-rich with low C/N ratios and high ^{15}N values (Figs 6 and 7; Table 1) was found in the surface mineral horizons of the intermediate aged (20–350 ky) chronosequence sites. Field observations indicate that preferential flow-paths facilitate movement of DOM into deeper soil horizons. In these SRO mineral rich soils, we observed numerous cracks and channels originating at the interface between the organic and surface mineral horizons that allow the direct movement of DOM from the O horizon to lower SRO-mineral rich B horizons (Chabbi *et al*., 2009; Marin-Spiotta *et al*., 2011). As a consequence there are two distinct pathways leading to OM accumulation in these soils: a near-surface incorporation of OM that has been strongly processed by microorganisms and a deeper injection of less strongly decomposed DOM along preferential flow-paths. In the latter case, C return to the atmosphere is retarded by its intimate association with SRO minerals.

Models of SOM formation often assume that C accumulates in soil because some of the C is highly recalcitrant due to it's chemical structure. Organo-mineral interactions are seldom explicitly included as a term, or as a stabilization mechanism. Although microbial decomposition of plant material contributed to the formation and transport of DOM from the organic horizons and to organic accumulation in the surface mineral horizons, our results indicate that the binding of carboxyl-rich aromatic DOM into SRO-organic complexes is the most likely explanation for the persistence of organic compounds in B horizons (Fig. 2a, b), in a manner similar to that described previously (Kaiser & Guggenberger, 2000; Kalbitz & Kaiser, 2008). In this case, the probable mechanism for organic C interaction with particle-surface bound metals is via inner-sphere complexation with Fe or Al in a heterogeneously bonded colloidal polymer (Chorover and Amistadi 2001; Mikutta *et al*., 2009) although aromatic pi-donor–acceptor interactions may also contribute in this case (Keiluweit & Kleber, 2009).

As discussed previously, SRO minerals are metastable and are formed in virtually all soils where Si, Al, and Fe containing primary minerals are being weathered. Andic soils rich in SRO minerals can form in non-volcanic parent materials such as granite, sandstone, and loess, depending on climate and vegetation (Supporting materials references). Dissolved organic matter production too is common to ecosystems where water supports microbial decomposition of organic substrates. Although the precise chemical composition of DOM varies as a function of abiotic and biotic factors such as climate, vegetation type or fire history, aromatic acids are a major constituent of DOM (Kalbitz *et al*., 2006). As a consequence, long-term carbon storage through retention of dissolved aromatic acids by reactive particles likely occurs in all SRO-mineral containing soils, although to a lesser extent than we demonstrate for volcanic soils here. Our results suggest that the amount of retention (Fig. 1) depends on sufficient rainfall and primary production, the availability of reactive OH sites on minerals and the C = O, COOH functional groups on DOM (Fig. 2a).

In the absence of reactive particle surfaces, and depending on the source from which it was derived, DOM may be subject to further microbial decomposition (Kalbitz *et al*., 2003; van Hees *et al*., 2005) or leaching from soil (Sanderman & Amundson, 2008) to riverine (Onstad *et al*., 2000) and subsequently marine environments (Hedges & Mann, 1979). Yet even very low concentrations of SRO minerals may bind and stabilize DOM in soil for long periods of time (Kaiser and Guggenberger 2000; Lilienfein *et al*., 2004; Masiello *et al*., 2004; Strahm & Harrison, 2009). Our results indicate that long-term storage in SRO minerals likely occurs via chemical retention with dissolved aromatic acids derived from plant litter.

Our study was conducted along a chronosequence, where vegetation inputs, climate, parent material and topography were well-constrained. Dissolved organic matter production was high across all sites under this humid climate regime while weathering in the intermediate aged sites favored the formation of short-ranged ordered minerals in the subsoil (Chorover *et al*., 1999, 2004). As shown in Fig. 1, many soils have at least small amounts of SRO minerals and their quantity is associated with increased carbon storage, however soils in different climate regimes can be expected to have different mechanisms involved in carbon compound preservation. For instance in Hawaii, in rainfall regimes wetter than that studied here, even where substantial

amounts of SRO minerals are present SOM may be more strongly stabilized through water logging, anoxia, and abundant production and preservation of organic matter as a consequence of reduced decomposition (Schuur *et al.*, 2001). Conversely sites with drier, more seasonal climates may be more limited by reduced dissolved organic matter production and a more unstable weathering (wet-dry cycling) environment that shortens the persistence of short-range ordered minerals (Chadwick & Chorover, 2001; Chadwick *et al.*, 2003; Ziegler *et al.*, 2003).

Implications for climate change

The increase in carboxyl functional groups observed in association with short-range order minerals suggests strong chemical binding (sorption) to reactive mineral surfaces, which would retard any direct response to perturbations such as climate change over decadal to centennial timescales. SRO mineral-stabilized carbon pools are less likely to decompose as a consequence of environmental or land-use change. However, if microbial activity increases in response to global warming (Davidson & Janssens, 2006) our results and other recent studies (Hagedorn *et al.*, 2008) suggest there could be a concomitant increase in the production of DOM from plant litter. In soils where high mineral dissolution rates are superimposed on continuous through-flux of oxidized plant components, high rates of C accumulation are likely to occur, thereby providing a large long-term C store.

Concluding remarks

Collectively, our results suggest that DOM comprised largely of aromatic acids accumulated preferentially with SRO minerals present in the subsoil. The correlation between aromatic acids and SRO minerals and the soil column sorption experiments suggest that binding (sorption) of DOM to reactive soil minerals via reactive OH sites is likely the dominant long-term retention mechanism. Given its high production, low bioavailability, and exceptional capacity to bond with soil minerals via carboxyl-rich functional groups, DOM comprised of oxidized aromatic plant compounds could be the principal source for long-term C storage in all soils where weathering of primary minerals produces SRO-minerals as metastable intermediate products.

Acknowledgments

We thank Russell Johnson, Dyke Andreasen, and Ping Yu for assistance during with the soil core experiment, stable isotope analysis, and NMR experiments. We thank Heraldo Farrington for assistance with sampling soils in the field. Soil column leaching experiments, sample preparation and analyses were conducted at the University of California, Santa Cruz and the Western Regional Research Center of PWA/ARS/USDA/EIW. This work was financially supported by National Research Initiative grant no. 2007-35107-18429 from the USDA National Institute of Food and Agriculture. Initial support was provided to the lead author by NASA Ames Research Center.

Author contributions

M.G. Kramer performed NMR and stable isotope analysis. J. Sanderman and M.G. Kramer designed, executed, and interpreted results from the organic and mineral soil core leaching experiment. J. Chorover provided valuable input and advice for the design of the soil column work. O.A. Chadwick provided soil mineralogy data. M.G. Kramer wrote the manuscript, to which all authors contributed substantial interpretation, discussion, and text.

References

Baldock JA, Masiello CA, Gélinas Y, Hedges JI (2004) Cycling and composition of organic matter in terrestrial and marine ecosystems. *Marine Chemistry*, **92**, 39–64.

Bäumler R, Caspari T, Totsche KU, Dorji T, Norbu C, Baillie IC (2005) Andic properties in soils developed from nonvolcanic materials in Central Bhutan. *Journal of Plant Nutrition and Soil Science*, **168**, 703–713.

Burt R. (2004) *Soil Survey Laboratory Methods Manual*. Soil Survey Investigations Report 4, 42, USDA-NRCS, Lincoln, NE, USA.

Buurman P, Peterse F, Almendros MA (2007) Soil organic matter chemistry in allophanic soils: a pyrolysis-GC/MS study of a Costa Rican Andosol catena. *European Journal of Soil Science*, **58**, 1330–1347.

Chabbi A, Kogel-Knabner I, Rumpel C (2009) Stabilised carbon in subsoil horizons is located in spatially distinct parts of the soil profile. *Soil Biology & Biochemistry*, **41**, 256–261.

Chadwick OA, Chorover J (2001) The chemistry of pedogenic thresholds. *Geoderma*, **100**, 321–353.

Chadwick OA, Gavenda RT, Kelly EF *et al.* (2003) The impact of climate on the biogeochemical functioning of volcanic soils. *Chemical Geology*, **202**, 195–223.

Chevallier T, Woignier T, Toucet J, Blanchart E (2010) Organic carbon stabilization in the fractal pore structure of Andosols. *Geoderma*, **159**, 16–7061.

Chorover J, Amistadi MK (2001) Reaction of forest floor organic matter at goethite, birnessite and smectite surfaces. *Geochimica et Cosmochimica Acta*, **65**, 95–109.

Chorover J, DiChiaro M, Chadwick OA (1999) Structural charge and cesium retention in a chronosequence of tephritic soils. *Soil Science Society of America Journal*, **63**, 169–177.

Chorover J, Amistadi MK, Chadwick OA (2004) Surface charge evolution of mineral-organic complexes during pedogenesis in Hawaiian basalt. *Geochimica et Cosmochimica Acta*, **68**, 4859–4876.

Clarke KR, Gorley RN (2006) *PRIMER v6: User Manual/Tutorial*. Primer-E Ltd, Plymouth, UK

Dahlgren RA, Saigusa M, Ugolini FC (2004) The nature, properties and management of volcanic soils. *Advances in Agronomy*, **82**, 114–183.

Dai KH, Johnson CE (1999) Applicability of solid-state 13C CP/MAS NMR analysis in Spodosols: chemical removal of magnetic materials. *Geoderma*, **93**, 289–310.

Davidson EA, Janssens IA (2006) Temperature sensitivity of soil carbon decomposition and feedbacks to climate change. *Nature*, **440**, 165–173.

Delvaux B, Strebl F, Maes E, Herbillon AJ, Brahy V, Gerzabek M (2004) An Andosol-Cambisol toposequence on granite in the Austrian Bohemian massif. *Catena*, **56**, 31–43.

Dijkstra P, LaViolette CM, Coyle JS, Doucett RR, Schwartz E, Hart SC, Hungate BA (2008) 15N enrichment as an integrator of the effects of C and N on microbial metabolism and ecosystem function. *Ecology Letters*, **11**, 389–397.

Guggenberger G, Kaiser K (2003) Dissolved organic matter in soil: challenging the paradigm of sorptive preservation. *Geoderma*, **113**, 293–310.

Hagedorn F, van Hees PAW, Handa IT, Hättenschwiler S (2008) Elevated atmospheric CO2 fuels leaching of old dissolved organic matter at the alpine treeline. *Global Biogeochemical Cycles*, **22**, 2.

Hedges JI, Mann DC (1979) The lignin geochemistry of marine sediments from the southern Washington coast. *Geochimica et Cosmochimica Acta*, **43**, 1809–1818.

van Hees PAW, Jones DL, Finlay R, Godbold DL, Lundström US (2005) The carbon we do not see–the impact of low molecular weight compounds on carbon dynamics and respiration in forest soils: a review. *Soil Biology and Biochemistry*, **37**, 1–13.

Hockaday WC, Masiello CA, Randerson JT, Smernik RJ, Baldock JA, Chadwick OA, Harden JW (2009) Measurement of soil carbon oxidation state and oxidative ratio by 13C nuclear magnetic resonance. *Journal of Geophysical Research, Biogeosciences*, **114**, G02014.

Igwe CA, Zarei M, Stahr K (2009) Colloidal stability in some tropical soils of southeastern Nigeria as affected by iron and aluminium oxides. *Catena*, **77**, 232–237.

Kaiser K, Guggenberger G (2000) The role of DOM sorption to mineral surfaces in the preservation of organic matter in soils. *Organic Geochemistry*, **31**, 711–725.

Kalbitz K, Kaiser K (2008) Contribution of dissolved organic matter to carbon storage in forest mineral soils. *Journal of Plant Nutrition and Soil Science*, **171**, 52–60.

Kalbitz K, Schmerwitz J, Schwesig D, Matzner E (2003) Biodegradation of soil-derived dissolved organic matter as related to its properties. *Geoderma*, **113**, 273–291.

Kalbitz K, Kaiser K, Bargholz J, Dardenne P (2006) Lignin degradation controls the production of dissolved organic matter in decomposing foliar litter. *European Journal of Soil Science*, **57**, 504–516.

Keiluweit M, Kleber M (2009) Molecular-level interactions in soils and sediments: the role of aromatic pi-systems. *Environmental Science and Technology*, **43**, 3421–1429.

Kirk TK, Farrell RL (1987) Enzymatic "combustion": the microbial degradation of lignin. *Annual Review of Microbiology*, **41**, 465–501.

Kleber M, Johnson MG (2010) Chapter 3: advances in understanding the molecular structure of soil organic matter: implications for interactions in the environment. *Advances in Agroecology*, **106**, 77–142.

Kögel-Knabner I, Guggenberger G, Kleber M *et al*. (2008) Organo-mineral associations in temperate soils: Integrating biology, mineralogy, and organic matter chemistry. *Journal of Plant Nutrition and Soil Science*, **171**, 61–82.

Kramer MG, Sollins P, Sletten RS, Swart PK (2003) N isotope fractionation and measures of organic matter alteration during decomposition. *Ecology*, **84**, 2021–2025.

Lilienfein J, Qualls RG, Uselman SM, Bridgham SD (2004) Adsorption of dissolved organic carbon and nitrogen in soils of a weathering chronosequence. *Soil Science Society of America Journal*, **68**, 292–305.

Marin-Spiotta E, Chadwick OA, Kramer M, Carbone MS (2011) Carbon delivery to deep mineral horizons in Hawaiian rainforest soils. *Journal of Geophysical Research*, **116**, G03011.

Martin JP, Haider K, Kassim G (1980) Biodegradation and stabilization after 2 years of specific crop, lignin, and polysaccharide carbons in soils, *Soil Sci. Journal of the American Society*, **44**, 1250–1255.

Masiello CA, Chadwick OA, Southon J, Torn MS, Harden JW (2004) Weathering controls on mechanisms of carbon storage in grassland soils. *Global Biogeochemical Cycles*, **18**, 1–9.

McDowell WH, Zsolnay A, Aitkenhead-Peterson JA *et al*. (2006) A comparison of methods to determine the biodegradable dissolved organic carbon from different terrestrial sources. *Soil Biology & Biochemistry*, **38**, 1933–1942.

Mikutta R, Schaumann GE, Gildemeister D *et al*. (2009) Biogeochemistry of mineral-organic associations across a long-term mineralogical soil gradient (0.3–4100 kyr), Hawaiian Islands. *Geochimica et Cosmochimica Acta*, **73**, 2034–2060.

Mikutta R, Kaiser K, Dörr N *et al*. (2010) Mineralogical impact on organic nitrogen across a long-term soil chronosequence (0.3–4100 kyr). *Geochimica et Cosmochimica Acta*, **74**, 2142–2164.

Nelson P, Baldock JA (2005) Estimating the molecular composition of a diverse range of natural organic materials from solid-state 13C NMR and elemental analyses. *Biogeochemistry*, **72**, 1–34.

Onstad GD, Canfield DE, Quay PD, Hedges JI (2000) Sources of particulate organic matter in rivers from the continental USA: lignin phenol and stable carbon isotope compositions. *Geochimica et Cosmochimica Acta*, **64**, 3539–3546.

Parfitt RL (2009) Allophane and imogolite: role in soil biogeochemical processes. *Clay Minerals*, **44**, 135–144.

Rasmussen C, Torn MS, Southard RJ (2005) Mineral assemblage and aggregates control carbon dynamics in a California conifer forest. *Soil Science Society of America Journal*, **69**, 1711–1721.

Rasmussen C, Matsuyama N, Dahlgren RA, Southard RJ, Brauer N (2007) Soil genesis and mineral transformation across an environmental gradient on andesitic lahar. *Soil Science Society of America Journal*, **71**, 225.

Sanderman J, Amundson R (2008) A comparative study of dissolved organic carbon transport and stabilization in California forest and grassland soils. *Biogeochemistry*, **89**, 309–327.

Sanderman J, Baldock JA, Amundson R (2008) Dissolved organic carbon chemistry and dynamics in contrasting forest and grassland soils. *Biogeochemistry*, **89**, 181–198.

Schilling M, Cooper WT (2004) Effects of chemical treatments on the quality and quantitative reliability of solid-state 13C NMR spectroscopy of mineral soils. *Analytica Chimica Acta*, **08**, 207–216.

Schoeneberger PJ, Wysocki DW, Behnam EC, Broderson WD (1998) *Field Book for Describing and Sampling Soils*. Natural Resources Conservation Service, USDA, National Soil Survey Center, Lincoln, NE, USA.

Schuur EAG, Chadwick OA, Matson PA (2001) Carbon cycling and soil carbon storage in mesic to wet Hawaiian montane forests. *Ecology*, **82**, 3182–3196.

Shevchenko SM, Bailey GW (1996) Life after death: lignin-humic relationships reexamined. *Critical Reviews in Environmental Science and Technology*, **26**, 95–153.

Sollins P, Homann P, Caldwell BA (1996) Stabilization and destabilization of soil organic matter: mechanisms and controls. *Geoderma*, **74**, 65–105.

Sollins P, Kramer MG, Swanston C *et al*. (2009) Soils of contrasting mineralogy: evidence for both microbial-and mineral-controlled soil organic matter stabilization. *Biogeochemistry*, **96**, 209–231.

Strahm BD, Harrison RB (2009) Controls on the sorption, desorption and mineralization of low-molecular-weight organic acids in variable-charge soils. *Soil Science Society of America Journal*, **72**, 1653–1664.

Stutzer A (1998) Early stages of podzolisation in young aeolian sediments, western Jutland. *Catena*, **32**, 115–129.

Torn MS, Trumbore SE, Chadwick OA, Vitousek PM, Hendricks DM (1997) Mineral control of soil organic carbon storage and turnover. *Nature*, **389**, 170–173.

Vitousek PM (2004), *Nutrient Cycling and Limitation: Hawai'i as a Model System*, Chapter 3–4, Princeton University Press, Princeton, NJ, USA.

Vitousek PM, Chadwick OA, Crews TE, Fownes JH, Hendricks DM, Herbert D (1997) Soil and ecosystem development across the Hawaiian Islands. *GSA Today*, **7**, 1–8.

Wada K (1989) Allophane and imogolite. In: *Minerals in the Soil Environment*, 2nd edn (eds Dixon JB, Weed SB), pp. 1051–1877. Soil Sci. Am., Book Series No. 1. ASA and SSSA, Madison, WI, USA.

Waksman SA, Tenney FG (1928) Composition of natural organic materials and their decomposition in the soil: III. The influence of nature of plant upon the rapidity of its decomposition. *Soil Science*, **26**, 38–75.

Weishaar JL, Aiken GR, Bergamaschi BA, Fram MS, Fujii R, Mopper K (2003) Evaluation of specific ultraviolet absorbance as an indicator of the chemical composition and reactivity of dissolved organic carbon. *Environmental Science and Technology*, **37**, 4702–4708.

Ziegler K, Hsieh JCC, Chadwick OA, Kelly EF, Hendricks DM, Savie SM (2003) Halloysite as a kinetically controlled end product of arid-zone basalt weathering. *Chemical Geology*, **202**, 461–478.

Supporting Information

Additional Supporting Information may be found in the online version of this article:

Table S1. Comparison of ^{13}C NMR regions obtaining using 50, 100, 200, and 300 Hz line broadening for a representative Bw soil sample.

Table S2. Comparison of ^{13}C CPMAS NMR Spectra (>30% observability) with direct polarization (DP) results (>85% observability). DP NMR results show that the aromatic carbon region (110–145) estimated by ^{13}C CPMAS is conservative. Soil samples are from the Pololu (350 ky) intermediate aged chronosequence site. The DOM sample is derived from Laupahoehoe organic soil horizons.

Additional references that report a positive Feo, Alo: C relationship for Fig 1 are included as supporting material.

Please note: Wiley-Blackwell are not responsible for the content or functionality of any supporting materials supplied by the authors. Any queries (other than missing material) should be directed to the corresponding author for the article.